Innovative High-Surface-Area CuO Pretreated Cotton Effective in Bacterial Inactivation under Visible Light

A. Torres,[†,‡] C. Ruales,[§] C. Pulgarin,*[,§] A. Aimable,[†] P. Bowen,[†] V. Sarria,[†] and J. Kiwi*[,||]

Department of Chemistry, Universidad de los Andes, Cra1E No 18A-10, Bogota, Colombia, EPFL-STI-IMX-LTP, Powder Technology Laboratory, Materials Institute, MXD 334, Station 12, Swiss Federal Institute of Technology, CH-1015 Lausanne, Switzerland, EPFL-SB-ISIC-GGEC, Station 6, Swiss Federal Institute of Technology, CH-1015 Lausanne, Switzerland, and EPFL-SB-ISIC-LPI, Station 6, Swiss Federal Institute of Technology, CH-1015 Lausanne, Switzerland

ABSTRACT This study presents the first report on enhanced bacterial inactivation of *E. coli* by RF-plasma pretreated cotton with high-surface-area CuO powders compared with nonpretreated cotton textiles. The high-surface-area CuO (65 m/g) powder was fully characterized. The *E. coli* inactivation proceeded in the dark and was accelerated under visible and sunlight irradiation even at very low levels of visible light irradiation. The effect the RF-plasma pretreatment of the cotton on the binding of CuO, applied light dose, the amount of CuO loading and initial *E. coli* concentration on the inactivation kinetics of *E. coli* is reported in detail.

KEYWORDS: RF-plasma • CuO high SSA • cotton • *E. coli;* visible light

INTRODUCTION

The manufacturing of high value added products such as bactericide textiles has increased rapidly in the past few years (1−5). This development also opened new interest in the pretreatment or activation of the surface of textiles by RF-plasma, vacuum-UVC light irradiation (6, 7), and corona discharge (8, 9) to deposit nanosized bactericide semiconductors and metals/metal-oxides. Bactericide textiles have been developed and intensively investigated recently by Daoud et al. (10, 11) and many other laboratories. Many bactericide agents have been applied on textiles like trichlosan, chitosan, N-halamine, polyhexamethylene, and peroxoacids (12), but poor efficiency and high toxicity besides leaching problems have made many of them unsuitable for long-term use (13). But silver has shown effective bacterial inactivation properties with low toxic impact to mammalian cells (13, 14). The bactericide properties of silver have been known for a long time. The effective of bactericide textiles remains for a long time with a sustained efficiency and the silver can be fixed on the textile without stabilizers (15, 16). Our group has recently reported the loading of Ag on different textiles like cotton, wool and polyester previously activated by RF-plasma and vacuum-UVC (17, 18). These studies indicated that the pretreatment of textile fibers by low pressure RF-plasma and Vacuum-UVC

increased the number of binding sites like: carboxylic acid −COOH, peroxides −O−O−, percarboxylic acids, epoxides, lactams and other giving raise to organic functional groups to bind Ag (6) or TiO$_2$ (7). These pretreatments roughens the textile surface also leading to (a) C−C bond scission, (b) decrease in the C−H bonds due to the destruction of intermolecular H-bonding, and (c) introduction of additional −C=O groups (as observed by XPS) having the effect of increasing the textile polarity and hydrophilicity which facilitates the adhesion between nanoparticles and the fabric (18).

The bactericide properties of Cu have been widely reported (19, 20). Recently, Borko and Gabbay (21) have reported bactericide, antiviral, algicide, and fungicide textiles that sustain well washing cycles loaded with CuO 1%. This textile is effective against *E. coli*, *Staphylococcus aureus*, and the *fungi Candida albicans.* These textiles are used in hospitals and laboratories using CuO against already-resistant antibiotics involving nosocomial infections and should not allow the development of resistant microbes, should be safe to humans, and do not cause skin irritation when applied externally (22, 23). Besides the known oxidation of organic pollutants in the dark or light (24, 25), recently our laboratory has reported the synthesis of large surface area CuO effective in the *E. coli* inactivation in the dark and under visible light (26, 27). The use of CuO textiles in external applications for skin treatments requires a stable, effective and long-lasting nanoparticle deposit of CuO for safe external applications. This point has been addressed describing CuO impregnated textiles with effective biocidal properties (28).

The present study addresses (a) the high-surface-area preparation and characterization of CuO, (b) the adhesion of the nanoparticulate CuO on the cotton activated by RF-
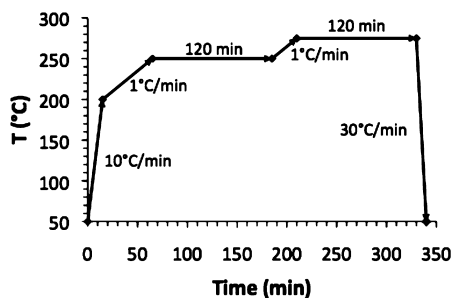
FIGURE 1. Thermal cycle for the Cu-oxalate decomposition under air (20 mL/min, 1 atm. P).

plasma in comparison with non plasma activated surfaces (6, 7), and (c) the evaluation of *E. coli* inactivation by cotton/CuO in the dark and under light.

EXPERIMENTAL SECTION

Reagents and Synthesis of High-Surface-Area CuO. Chemicals $Cu(NO_3)_2 \cdot 3H_2O$, $Na_2C_2O_4$, Merck reagents and hydroxypropyl-methylcellulose (HPMC 100, M_w 64 000 g/mol, Hercules GmbH) were pro-analysis (p.a.) and used as received. $Cu(NO_3)_2$ and $Na_2C_2O_4$ solutions were prepared in ultrapure water previously boiled to eliminate dissolved CO_2. These solutions were then filtered at 0.2 μm to eliminate dust. The stock solutions were stored in closed vessels to avoid further contamination.

For the preparation of the large-surface-area CuO powders, $Cu(NO_3)_2$ and $Na_2C_2O_4$ (0.02 M) solution were prepared just before use to avoid CO_2 contamination and mixed in a 5 L batch under vigorous stirring (1500 rpm) for 30 min and subsequently aged for 2 h as shown in reaction 1

$$Cu^{2+} + 2NO_3^- + 2Na^+ + C_2O_4^{2-} \leftrightarrow CuC_2O_4 + 2NaNO_3 \quad (1)$$
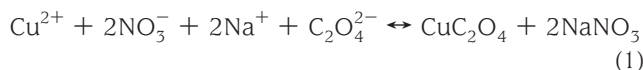
The Cu-oxalate was then collected by filtration using 0.2 μm filters and dried 24 h at 70 °C. The thermal decomposition of Cu-oxalate into copper oxide was carried out in a tubular furnace (Linderberg) under airflow (20 mL/min). The temperature profile of the process is shown in Figure 1. This treatment avoids overheating due to the furnace inertia and provides an accurate control of the temperature as required in the synthesis of high-surface-area CuO (29).

The CuO (65 m²/g) was deposited on bleached cotton received from Cilander AG, Cilanderstr.17, CH-9101, Herisau. The cotton samples (2 × 2 cm) were fist activated by RF- plasma source from Harrick Corp, UK with a generator source of 13.56 MHz, 100W at a pressure of 1 Torr for 30 min. This pretreatment introduced additional carboxylates, percarboxylates, epoxides, lactams, polyphenols, and peroxide groups on the cotton surface giving raise additional binding sites for CuO (6, 7).

Then, the samples were immersed in a sonicated solution of CuO (0.2 g/mL) and heated for 1 h at 75 °C. The loading of the samples was completed in three steps: (a) first heating at 60 °C for 1 h, (b) followed by heating at 100 °C for 15 min, and finally (c) the loose CuO was sonicated out of the samples in distilled water for 5 min followed by drying at 60 °C.

Thermogravimetric Analysis of CuO. The thermogravimetric analysis (TGA) of the oxalate decomposition was followed up to 600 °C airflow with a heating rate of 10 °C/min in the TGA, Mettler TGA/DSC/TMA analyzer.

X-ray Diffraction of CuO (XRD). The phase identification was carried out by means of an X-ray powder diffraction X'Pert diffractometer, Philips Cu–Kα radiation. To determine the size of the primary crystallite, we applied the Scherer equation (see

eq 2). The instrumental broadening was determined using alumina for large crystal sizes >1 μm.

$$d_{XRD} = (K\lambda_X)/(\beta_{Xp}\cos(\theta)) \quad (2)$$

Where K is equal to 0.9, λ_X is the X-ray (wavelength 1.54 Angstrom), β_{Xp} is the integral breadth of the material (30), calculated using $\beta_{Xp} = \sqrt{(\beta^2 - \beta^2 \text{ alumina})}$.

Specific Surface Area (SSA) and Particle Size Distribution. The Brunauer–Emmett–Teller (BET) specific surface areas S_{BET} (m²/g) were determined from N_2 adsorption isotherms (Micromeritics Gemini 2375) for the oxalate and CuO powders. The size of the primary particles, d_{BET} (nm) was calculated by assuming spherical monodisperse particles in eq 3, where ρ was the density of the oxalate $\rho_{oxalate} = 3.5$ g/cm³ and the density of the oxide $\rho_{oxide} = 6.5$ g/cm³

$$d_{BET} = 6/(S_{BET}\rho) \quad (3)$$

The oxalate was dried before the SSA experimental determinations at 110 °C in N_2 for 1 h, and the CuO was dried at 200 °C. The particle size distribution (PSD) was collected using a laser diffraction method (Malvern Mastersizer S, $\rho = 6.5$ g/cm³ and $n = 2.6$) by dispersing the CuO powder in a solution of poly(acrylic acid) 0.1 wt %, $R = 1.5$ (pH ~10).

Electron Microscopy (SEM) and X-ray Fluorescence Determination of Cu on Textiles. The powder morphology was analyzed by scanning electron microscopy (SEM, Philips XL 30 FEG microscope). The SEM sample was prepared by dispersing the powder in ethanol. One drop of the suspension was then deposited on an Al-support and dried in air. The spectrometer used was an RFX, PANalytical PW2400. By this technique each element emits an X-ray of a certain wavelength associated with its particular atomic number.

Irradiation of Cotton/CuO Samples during *E. coli* Inactivation. Figure 6 shows in the insert the visible emission spectrum of the Osram Lumilux T8-L18W lamp (Winterthur, Switzerland) used to activate the cotton/CuO, having each lamp an output of 1.2 mW/cm². Figure 10 shows the results for *E. coli* bacterial inactivation mediated by a Suntest solar simulator CPS (Atlas GmbH) equipped with a Xe-lamp (830 W). This source has a spectral distribution with 0.5 % of the photons at wavelengths <300 nm, and 7 % between 300 and 400 nm and this is shown in the insert to Figure 10. The light intensity was set at 27 mW/cm².

Bacterial Inactivation under Light and in the Dark. The bacterial strain *Escherichia coli* K12 was inoculated in 5 mL of Luria–Bertani solution and grown during 8 h at 37 °C with constant agitation under aerobic conditions. Aliquots of the overnight culture were inoculated into a fresh medium and incubated aerobically at 37 °C for 15 h. At the stationary growth phase, bacteria cells were collected by centrifugation at $500g$ for 15 min at 4 °C and the bacterial pellets were washed three times and resuspended in a NaCl/KCl solution.

The bactericide activity of cotton/CuO was tested on *E. coli* sterilizing 2 cm² of cotton/CuO and cotton samples by autoclaving at 121 °C for 2 h. Then, 20 μL aliquots of the culture in NaCl/KCl solution were added to the cotton/CuO and cotton samples to adsorb the bacteria before irradiation. Next, the samples were transferred into a sterile 2 mL Eppendorf tube containing 1 mL of autoclaved NaCl/KCl saline solution and mixed thoroughly using a vortex for 3 min. Serial dilutions were made in NaCl/KCl solution. One-hundred microliters of each aliquot was spread on the nutrient agar plate. Agar plates were incubated at 37 °C for 24 h before counting the CFU. Experiments were replicated at least two times and in some cases
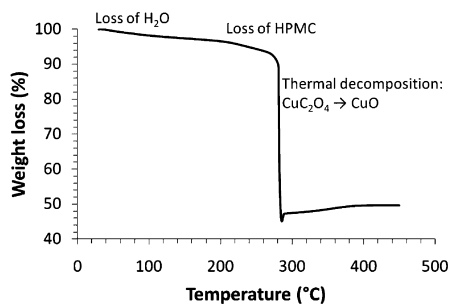
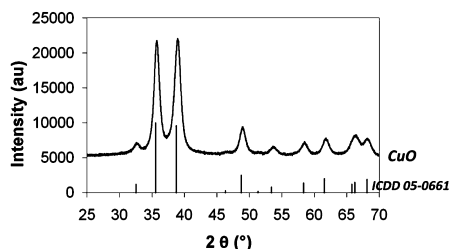FIGURE 2. TGA curve of Cu-oxalate powder (heating rate 10 °C/min, air).

FIGURE 3. XRD of CuO (65 m²/g) from Cu-oxalate assigned to the XRD of tenorite form (ICDD 05−0661).
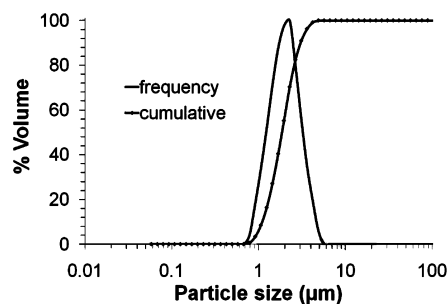

FIGURE 4. Particle size distribution measured by laser diffraction (Malvern Mastersizer) for CuO (65 m²/g).
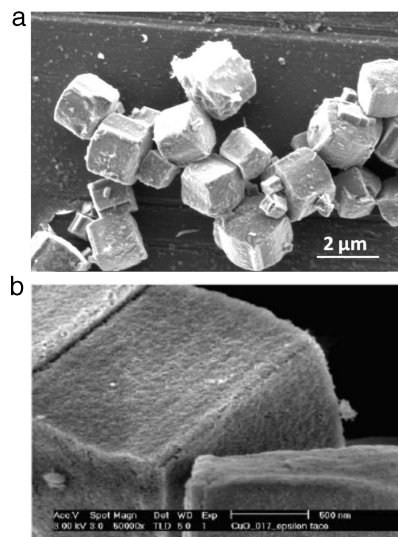

FIGURE 5. (a) SEM of CuO powders having 65 m²/g. (b) SEM of CuO showing the detailed structure of the cubic crystallites

three times. The experimental points in Figures 6−10 were an average of the experimental data. The recovery percentage by the experimental method used was 91.7 ± 2.7%.

RESULTS AND DISCUSSSION

Thermogravimetry of Cu-oxalate. The TGA curve of the Cu-oxalate powder is shown in Figure 2 showing three steps. The weight loss between 30 and 200 °C can be attributed to adsorbed water followed by a step between 200 and 275 °C due to the decomposition of the polymer hydroxypropyl-methylcellulose (HPMC). The third step beginning at 275 °C shows the rapid weight loss due to the decomposition of the Cu-oxalate into the CuO. The oxalate route followed a very slow and controlled thermal decomposition in air. This was the best route to obtain microsize particles of CuO with a reproducible high specific surface area and controlled morphology (see SEM in Figure 5).

X-ray Diffraction, Surface Specific Area (SSA), and Mean Aggregate (d_{v50}) Size of CuO Powders. Figure 3 shows the X-ray diffraction on of CuO obtained from the Cu-oxalate as described in Reagents and Synthesis of high-surface-area CuO in the Experimental Section. Relation 2, based on the XRD, determined the size of the primary crystallite at 13 nm. This agrees with the value of 12 nm estimated from relation 3 above for the single particle size of CuO from the SSA measurements. The particle size distribution (PSD) is presented in Figure 4 and the median size of the aggregate was 1.85 μm was observed implying a high porosity being present in the CuO.

Scanning Electron Microscopy of CuO (SEM). From the SEM picture in Figure 5a, we could observe the morphology of the CuO powder, composed of cubic particles around 2 μm in size. The narrow particle size distribution measured by laser diffraction in Figure 4 confirms the narrow size distribution observed by SEM and the median size measured of d_{v50} =1.85 μm, as observed in Figure 5a.

Figure 5b presented the SEM of CuO powders having 65 m²/g shows the detailed structure of the cubic crystallites. If we take the known relation for the size of the CuO particle $d_{BET} = 6000 /(S_{BET}\rho)$, where BET is the specific surface area of CuO (65 m²/g) and ρ is the CuO density (6.5 g/cm³). This allows us to estimate that the primary particle size d_{BET} is ∼14 nm in the nanometer range.

***E. coli* Inactivation by Cotton/CuO (65 m²/g) under Visible Light Irradiation.** The beneficial effect of the RF-plasma on the cotton surface introducing additional binding sites can be seen in Figure 6. Figure 6 presents the *E. coli* K12 bacterial inactivation of cotton/CuO (65 m²/g) samples. Trace a shows a negligible decrease of *E. coli* on cotton in the dark on samples not activated by RF-plasma because little CuO sticks to the cotton surface. Trace b shows an increased *E. coli* inactivation within 4 h due to the highly oxidative species generated by CuO under light. The mechanism is described in the next section below. The additional binding sites introduced by RF-plasma on the cotton binds more CuO, increasing the bacterial inactivation in the dark and under light as shown in traces c and d, respectively.

The mechanism of *E. coli* inactivation in the dark by RF-plasma CuO-loaded cotton samples in Figure 6e can be understood by the findings reported by our previous work (27). After the CuO is contacted with the bacterial suspension
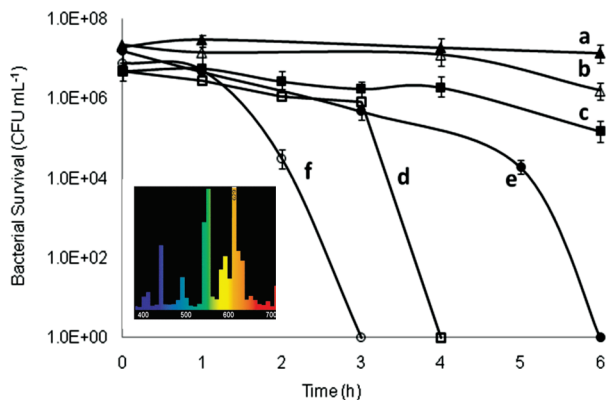
FIGURE 6. *E. coli* inactivation: (a) cotton alone, dark; (b) cotton under visible light irradiation from an Osram Lumilux T8-L18W source with 5 lamps (4.7 mW/cm²); (c) cotton/CuO(65 m²/g), (0.71%wt/wt), dark; (d) cotton/CuO(65 m²/g), (0.71 wt %/wt), under visible light irradiation from an Osram Lumilux T8-L18W source with 5 lamps (4.7 mW/cm²); (e) RF-plasma cotton/CuO(65 m²/g), (071 wt %/wt), dark; (f) RF-plasma cotton/CuO(65 m²/g), (0.71 wt %/wt), under visible light irradiation from an Osram Lumilux T8-L18W source with 5 lamps (4.7 mW/cm²). The inset shows the wavelength distribution of the Osram Lumilux T8-L18W lamp used in the bacterial inactivation.
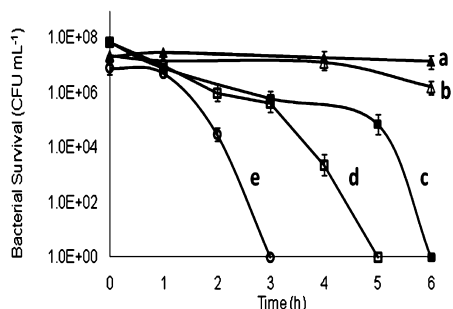

FIGURE 7. *E. coli* inactivation mediated by: (a) cotton alone, dark; (b) cotton under visible light irradiation from an Osram Lumilux T8-L18W source with 5 lamps (4.7 mW/cm²); (c) RF-plasma cotton/CuO, (65 m²/g) with a loading of 0.71 wt %/wt in the dark (■); (d) same as in c but under light irradiation of 1 lamp (1.2 mW/cm2) (□); (e) same as in d under light irradiation of 5 lamps (4.7 mW/cm²) (○).

prepared in buffered solutions, some remarkable spectral changes were observed by XPS. The surface of CuO exposed to bacterial suspension almost completely changes its oxidation state from Cu^{2+} to Cu^{1+}. Decomposition of the Cu $2p_{3/2}$line reveals that the outermost layer of the catalyst becomes 80 % in Cu_2O and only 20 % remains as CuO. The evidence for this observation is the shift in the Cu $2p_{3/2}$and Cu $2p_{1/2}$lines positioned initially at 933.7 and 953.6 eV to 932.6 and 952.6 eV, respectively for catalysts contacted with *E. coli* in the dark. Moreover, the concomitant disappearance of the Cu^{2+} shakeup satellite lines at 942.3 and 962.2 eV indicated that transformation of CuO to Cu_2O is taking place. Hence, the catalyst surface is almost immediately reduced after the CuO contacts the bacteria and remains in reduced state within the 4 h of dark reaction as shown in Figure 6, trace e.

Figure 7 shows the *E. coli* inactivation as a function of the applied light intensity. The bacterial inactivation time decreases as the intensity of the applied visible light was increased from 1.2 mW/cm² (1 lamp) to 4.7 mW/cm² (5 lamps).
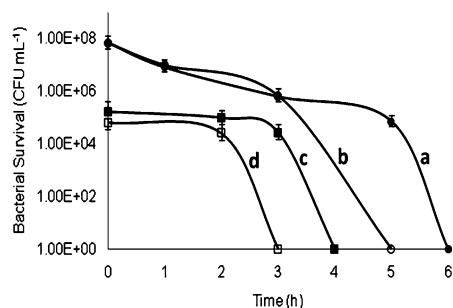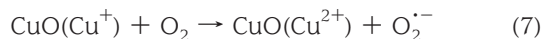

FIGURE 8. *E. coli* inactivation under visible light (4.7 mW/cm²), RF-plasma cotton/CuO(65 m²/g) as a function of amount of Cu deposited on the cotton: (a) CuO (0.71 wt %/wt), dark (•); (b) CuO (0.71 wt %/wt), light (○); (c) CuO (0.78 wt %/wt), dark (■); (d) CuO (0.78 wt %/wt), light (□).
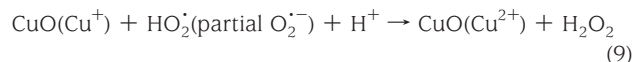
Reaction Mechanism of CuO under Illumination.

The semiconductor character of CuO has been recently described (27). The main features are presented below. Under irradiation, CuO leads to oxidative radicals by a mechanism

$$CuO + h\nu(<720 \text{ nm}) \rightarrow CuO(e_{cb}^-, h_{vb}^+) \qquad (4)$$
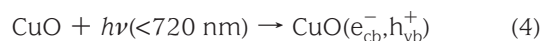
The e_{cb}^- in eq 4 is produced from the CuO (p-type) with a band gap energy of 1.72 eV, a flat-band potential of −0.3 V SCE (pH 7) and a valence band at +1.4 V SCE (26). The electron−hole pair is formed with photon energies exceeding the band gap of CuO. The excited electron could either react (a) directly with the O_2 forming $O_2^{\bullet-}$ (reaction 5) or by (b) reducing the Cu^{2+} lattice to Cu^+, leading to ensuing reactions 6 and 7 with formation of $O_2^{\bullet-}$ radicals

$$CuO(e_{cb}^-) + O_2 \rightarrow CuO + O_2^{\bullet-} \qquad (5)$$

$$CuO(e_{cb}^-) \rightarrow CuO(Cu^+) \qquad (6)$$

$$CuO(Cu^+) + O_2 \rightarrow CuO(Cu^{2+}) + O_2^{\bullet-} \qquad (7)$$

Equation 8 shows the equilibrium between H^+ and $O_2^{\bullet-}$ leads to the formation of the $HO_2^\bullet$ radical. The $HO_2^\bullet$ stated in eq 8 leads to the production of adsorbed H_2O_2 in CuO eq 9

$$H^+ + O_2^- \leftrightarrow HO_2^\bullet(\text{partial } O_2^{\bullet-}) \ pK_a = 4.8 \qquad (8)$$

$$CuO(Cu^+) + HO_2^\bullet(\text{partial } O_2^{\bullet-}) + H^+ \rightarrow CuO(Cu^{2+}) + H_2O_2 \qquad (9)$$

with $k_8 = 0.6-2.3 \text{ M}^{-1} \text{ s}^{-1}$ (34).

Inactivation of *E. coli* As a Function of the CuO Content on the Cotton Textile.

Figure 8 presents the inactivation of *E. coli* as a function of the amount of CuO/cm² on the cotton surface. Trace 8a shows the bacterial inactivation with a sample cotton/CuO (0.71 % Cu wt/wt) in
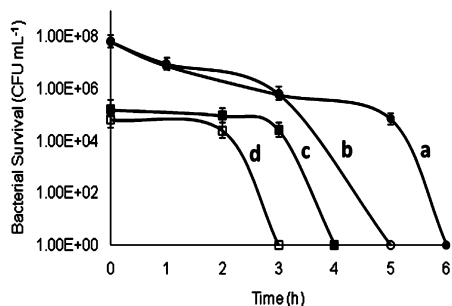
FIGURE 9. Bacterial inactivation, RF-plasma cotton/CuO(65 m^2/g) (0.71 wt %/wt), under visible illumination as a function of initial number of *E. coli*, 1 lamp (1.2 mW/cm^2): (a) dark (•), (b) light (○), (c) dark (■), (d) light (□).

the dark and trace 8b shows the faster inactivation of *E. coli* by the same cotton/CuO sample under visible light. The beneficial effect on the *E. coli* inactivation by CuO under band gap irradiation because of its semiconductor behavior has been described in the previous section. Trace 8d for a cotton sample having a higher CuO loading of 0.78 % Cu wt/wt inactivated under visible light irradiation the *E. coli* within 3 h. The *E. coli* inactivation kinetics is the same as found for the sample with a lower loading of (0.71 % Cu wt/wt) in shown in trace 8b. This means that above a certain loading of Cu, the *E. coli* inactivation kinetics does not strongly depend on the amount of CuO on the cotton within CuO range screened in this study. This result is meaningful in the following context: In the way we prepare the CuO suspensions from the CuO (65 m^2/g), we tried several ways to vary in a wider range the CuO loading of the cotton aiming at relative short times for *E. coli i*nactivation. But only the loading range of 0.70−0.80 % Cu wt/wt an acceptable *E. coli* inactivation kinetics was observed, and higher loadings did not lead to an improved *E. coli* inactivation kinetics.

Bacterial Inactivation Kinetics As a Function of the Initial Amount of *E. coli.* Figure 9 shows the *E. coli* inactivation kinetics for two different initial bacterial concentrations on cotton/CuO (65 m^2/g) in the dark and under light. The lowest visible light intensity of 1.2 mW/cm^2 (1 lamp) was applied. This light intensity used was is about 1 % of the full sunlight intensity (AM 1) and this low light intensity was seen to have a significant effect enhancing bacterial inactivation. As noted in the captions in Figure 9, the *E. coli* inactivation kinetics increases when visible light is applied and also becomes faster as expected when the initial concentration of *E. coli* decreases.

Inactivation of *E. coli* under Suntest Light Irradiation: Test of Commercial CuO. Figure 10 presents the results of the bacterial inactivation for *E. coli* starting with a higher bacterial concentration of 1 × 10^{10} CFU/mL in the dark and under light. Traces a and b present the bacterial inactivation by cotton in the dark and under light. The increased activity of the cotton under sunlight with a dose of 27 mW/cm^2 is probably due to the tensides, bacterial amylase, networking agents, stabilizer, and organic peroxides added in the finishing steps in cotton fabrics ready for use. These additives generate under light intermediates and radicals leading with bactericide action (33). The light
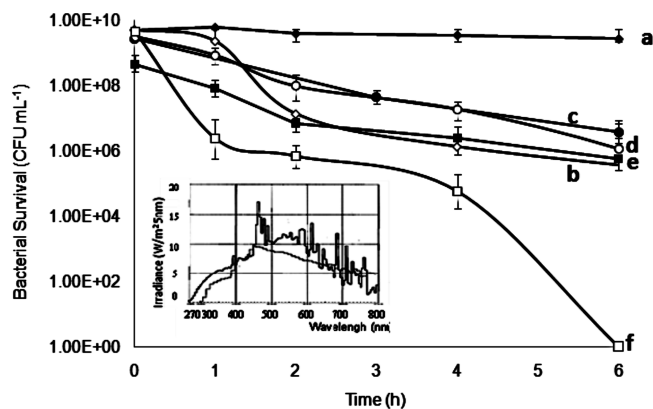

FIGURE 10. *E. coli* inactivation under Suntest simulated radiation (27 mW/cm^2): (a) cotton, dark (♦); (b) cotton, light (◇); (c) RF-plasma cotton/CuO commercial (1 m^2/g), dark (•); (d) RF-plasma cotton/CuO commercial(1 m2/g), light (○); (e) Rfplasma cotton/CuO(65 m2/g), dark (■); (f) RF-plasma cotton/CuO(65 m^2/g), light (□). The insert shows the wavelength profile of the Suntest lamp.

intensity used in Figure 10 is about 6 times bigger than the light intensity used in Figure 6 and this is probably the cause for the *E. coli* partial inactivation under light shown in trace b compared to the almost negligible effect of light on cotton shown in Figure 6. Trace c confirms that the RF-plasma pretreated cotton loaded with commercial low-surface-area CuO (1 m^2/g) was more active than pure cotton in the dark and the activity also increased under light as expected. The last two traces, e and f, show the significant higher bacterial inactivation of *E. coli* by pretreated cotton loaded with high surface area CuO (65 m^2/g) in the dark and even more under light because of the light irradiation on the CuO band gap.

The CuO having 65 m^2/g has a particle radius of 13 nm as determined by the SSA measurements. If we take spherical geometry for these particles, the sphere has a surface of 2 × 10^3 nm^2 and for the 65 m^2/g there would be 3.3 × 10^{16} sites/g CuO.

A rough estimation can be made for the amount of CFU inactivated by one photon. In our experiments we used 20 μL of a sample of *E. coli* 10^3 CFU/mL on 4 cm^2 cotton/CuO and applied for 6 h Suntest light emitting 2 × 10^{17} photons/cm^2/s to inactivate completely the bacteria. We estimate that around 7 CFU were inactivated per incident photon. The high number of CFU inactivated per incident photon may be due to three factors: (a) the secondary reactions on the cotton leading to *E. coli* deactivation, (b) chain reactions occurring during the bacterial inactivation process, and (c) the hot-electrons produced during the cotton RF-pretreatment.

CONCLUSIONS

• The first report is presented for cotton/CuO modified bactericide textiles using large surface area CuO with enhanced adhesion of the CuO due to the RF-plasma treatment. The RF-plasma pretreatment introduces additional binding sites on the cotton with beneficial effects on the *E. coli* inactivation.

• This work reports on the preparation method and characterization of large surface area CuO nanoparticles.

• The present findings indicate that low intensity visible light with about 1 % of the full solar irradiation had a

significant effect on the inactivation of *E. coli* mediated by CuO powders.

REFERENCES AND NOTES

(1) Yuranova, T.; Rincon, G. A.; Laub, D.; Kiwi, J. *Catal. Today* **2007**, *122*, 109–117.

(2) Kiwi, J.; Pulgarin, C. *Catal Today.* **2010**, *151*, 2–7.

(3) Ilic, V.; Saponjic, Z.; Vodnik, V.; Mihailovic, D.; Jovancic, P.; Nedeljkovic, J.; Radetic, M. *Fiber Polym.* **2009**, *10*, 650–657.

(4) Melaiye, A.; Sun, Z.; Hindi, K.; Milstedt, A.; Ely, D.; Reneker, D.; Tessier, C.; Youngs, W. *J. Am. Chem. Soc.* **2005**, *127*, 2285–2291.

(5) Mills, A; LeHunte, S. *J. Photochem. Photobiol., A* **1997**, *108*, 1–35.

(6) Yuranova, T.; Rincon, G. A.; Bozzi, A.; Parra, S.; Pulgarin, C.; Albers, P.; Kiwi, J. *J Photochem. Photobiol., A* **2003**, *161*, 27–34.

(7) Bozzi, A.; Yuranova, T.; Kiwi, J. *J. Photochem. Photobiol., A* **2005**, *172*, 27–34.

(8) Radetic, M.; Ilic, V.; Vodnik, V.; Dimitrijevic, S.; Jovancic, P.; Saponjic, S.; Nedelkovic, J. *Polym. Adv. Technol.* **2008**, *19*, 1816–1821.

(9) Ilic, V.; Saponjic, Z.; Vodnic, V.; Molina, R.; Dimitrijevic, S.; Jovancic, P.; Nedelkovic, J. *J. Mater. Sci.* **2009**, *44*, 3983–3989.

(10) Ki, K.; Chen, X.; Liu, L.; Xin, J.; Mak, C.; Daoud, A. W. *J. Mater. Chem.* **2007**, *17*, 3504–3510.

(11) Daoud, W. A.; Xin, J. H.; Zhang, Y. H. *Surf. Sci.* **2005**, *599*, 6975.

(12) Tung, W. S.; Daoud, W. A. *J. Colloid Interface Sci.* **2008**, *326*, 283–290.

(13) Gao, Y.; Cranston, R. *Text. Res. J.* **2005**, *78*, 60–66.

(14) Czajka, R. *Fiber Text. East Eur.* **2005**, *13*, 13–16.

(15) Alt, V.; Bechert, T.; Steinrucke, P.; Wegener, M.; Schnettler, R. *Biomaterials* **2004**, *25*, 4383–4391.

(16) Lee, H.; Jeong, H. *Textile Res., J.* **2005**, *75*, 551.

(17) Yuranova, T.; Rincon, G. A.; Pulgarin, C.; Laub, D.; Xanthopoulos, N.; Mathieu, H.-J.; Kiwi, J. *J. Photochem. Photobiol., A* **2006**, *181*, 363–369.

(18) Kasanen, J.; Suvanto, M.; Pakkanen, T. *J. Appl. Polym. Sci.* **2009**, *111*, 2597–2603.

(19) Karlin, D. K.; Gulneth, Y. In *Progress in Inorganic Chemistry*; Lippard, S. J., Ed.; Wiley: New York, 1987; Vol. 35, pp 220–237.

(20) Hostynek, J.; Maibach, I. *Rev. Environ. Health* **2003**, *18*, 153–183.

(21) Borkow, G.; Gabbay, J. *FASE* **2004**, *18*, 1728–1730.

(22) Borkow, G.; Gabbay, J. *J Med. Hypothesis* **2008**, *70*, 990–994.

(23) Malnick, S.; Bardenstein, R.; Huszar, M.; Gabbay, J.; Borkow, G. *J. Hosp. Infect.* **2008**, *70*, 89–92.

(24) Bandara, J.; Kiwi, J.; Pulgarin, C.; Peringer, P.; Pajonnk, G.-M.; Elaloui, A.; Albers, P. *Env. Sci. Technol* **1996**, *20*, 1261–1267.

(25) Moshe, T.; Dror, T.; Berkowitz, T. *Appl. Catal., B* **2009**, *85*, 207–212.

(26) Bandara, J.; Bowen, P.; Soare, L.; Jardim, W.; Kiwi, J. *Langmuir* **2005**, *21*, 8554–8559.

(27) Paschoalino, M.; Guedes, N.; Jardim, W.; Mielczarski, E.; Mielczarsi, J.; Bowen, P.; Kiwi *J. Photochem. Photobiol., A* **2008**, *199*, 105–111.

(28) Gabbay, J.; Mishal, J.; Magen, E.; Zatcoff, R. C.; Shemer-Avni, Y.; Borkow, G. *J. Ind. Text.* **2006**, *35*, 323–35.

(29) Jongen, N.; Hoffmann, H.; Bowen, P.; Lemaitre, L. J. *Mater. Sci. Lett.* **2000**, *19*, 1073–1075.

(30) Balzar, D.; Audebrand, N.; Daymond, M.; Fitch, M.; Hewat, A.; Langford, J.; Le Bail, A.; Louer, B.; Mason, O., Toby, B. http://journals.iucr.org/j/issues/2004/086/00/ks0213/ks0213hdr.html.

(31) Bowen, P. *J. Dispersion Sci. Technol.* **2002**, *23*, 631–640.

(32) ISO Standard 20743, Sept 2007, Evaluation of the antibacterial activity of biocidal products (www.afnor.org).

(33) Cilander A. G., private communication.

(34) Goldstein, S.; Czapski, G.; Meyerstein, D. *J. Am. Chem. Soc.* **1990**, *112*, 6489–6493.

AM100370Y